Performance Assessment of Concentrated Photovoltaic Thermal (CPVT) Solar Collector at Different Locations

Sahand Hosouli[1], Diogo Cabral[2], João Gomes[1], George Kosmadakis[3], Emmanouil Mathioulakis[3], Hadi Mohammadi[1], Alexander Loris[1], Adeel Naidoo[1]

[1] MG Sustainable Engineering AB, Uppsala (Sweden)

[2] University of Gävle, Gävle (Sweden)

[3] Solar & Other Energy Systems Laboratory, National Centre for Scientific Research "Demokritos", Agia Paraskevi (Greece)

Abstract

The double MaReCo (symmetric reflector geometry) solar collector (DM-CPVT) has been designed and developed by MG Sustainable Engineering AB (MG) and the University of Gävle (HiG). Performance and overall electrical and thermal parameters of the collector have been studied and presented. The outdoor tests have been performed in both Sweden during the summer months of 2020 and Greece in September of 2020. The goal of the studied designs is to optimize the incoming solar radiation that can be collected without the need for tracking. This is possible due to the use of a symmetric reflector geometry with low concentration factor and lower collector depth. The use of a symmetric reflector geometry allows higher annual outputs worldwide. Furthermore, a low concentration factor is necessary to avoid tracking and a lower collector depth to reduce the shading, which is particularly important for the electrical production of these DM-CPVT design concepts. The testing facilities in both locations are also described in this paper. The information on the thermal performance of a collector is important for the prediction of the energy output of any solar system. The thermal properties assessment of the DM-CPVT collector followed the procedures of the ISO 9806:2017 standard and reported. The outdoor testing results have been validated with a deviation of 2.8% and 2.4% for both thermal and electrical peak efficiencies between the testing facilities, respectively. Regarding the Incidence Angle Modifier testing results, the deviation is negligible for all angles of incidence, which shows that outdoor testing procedures can be fairly accurate when tracking systems are not available.

Keywords: CPVT, DM-CPVT, Solar Collector Testing

1. Introduction

The active application of solar energy technologies relies mainly on the use of solar thermal (ST) systems for heat generation and photovoltaic (PV) systems for electricity generation. The low surface power and energy density of PV modules, combined with the relatively low exergy of the solar flat plate thermal collectors, and the limited available ground area can be overcome by higher combined electrical and thermal (per unit area) efficiencies of a solar photovoltaic-thermal (PVT) system (Dwivedi et al. 2020; Kenny et al. 2003). A PVT collector is able to generate electricity and heat from the same area and is a single unit formed by a combination of PV and solar thermal technologies (Gomes et al. 2014; Zhang et al. 2012). PVT collectors have several applications in residential and industry such as, solar drying, water desalination, water and space heating, solar cooling, building integrated skins façades, etc. (Charron and Athienitis 2006; Sultan and Efzan 2018).

In recent years, several studies on PVT have been published. (Aste et al. 2016) presents a mathematical model for energy simulation of PVT systems in three different locations. (Keizer et al., 2016) stated that the efficiency of a PVT system is significantly high when comparing with PV systems. (Proell et al. 2016) investigates the performance of the PV systems and reports that these systems only convert 10-20% of the incoming solar radiation in electricity. Part of the remaining absorbed radiation can be converted to heat by a PVT collector. Furthermore, PV temperatures can potentially be reduced, thereby increasing the electrical yield. PVT collectors improve thermal efficiency by concentrating sunlight with CPC reflectors, allowing for more solar thermal applications. (Lämmle et al. 2017) findings show that the highest overall yields and the optimum energetic usage of the collector surface area are achieved by thermally optimized glazed PVT collectors with low-emissivity coatings. When compared to a side-by-side installation of flat plate collectors and PV modules with comparable thermal output, these collectors provide up to three times the electrical output. (Tomar, Tiwari, and Bhatti 2017) studies highlight that, improving the overall thermal efficiency of a PVT collector with the integration of an air duct behind the photovoltaic module enhances the overall thermal efficiency of the collector by extracting the excess heat released by the modules.

Selection and/or peer review under responsibility of Scientific Committee
doi:10.18086/swc.2021.22.05 Available at http://proceedings.ises.org

(Joshi and Dhoble 2018b) research reveals the concept of PVT systems is almost five decades old. But still, the technology is not much commercialized. (Maatallah, Zachariah, and Al-Amri 2019) reports that, from a financial standpoint and overall exergy basis, the payback period for the water-based PVT-PCM system is roughly 6 years, which is 11.26 % shorter than for traditional PV panels. In addition, when compared to traditional PV panels, the water-based PVT-PCM system has a long-term lifespan conversion efficiency of roughly 27%. (Guarracino et al. 2019) reports that the electrical and economic performance of PVT systems is highly dependent on various design and operational considerations such as materials and geometry. All these findings are showing how photovoltaic-thermal (PVT) solar collectors can achieve higher combined electrical and thermal (per unit area) efficiencies. The thermal coupling of PV cells with solar thermal absorbers enhances the thermal energy harvesting through a heat transfer cooling (HTF) fluid that not only cools down the PV cells below the operating temperature of standard PV modules but also improves electrical performance. The PVT thermal performance is often assessed using ISO 9806:2017 as the international standard for solar thermal collectors, and electrical performance is evaluated by IEC standards. Furthermore, PVT solar collectors can apply for Solar Keymark certification under particular rules, in which the thermal performance is measured using synchronous thermal and electrical generation under maximum power point conditions, as the heat and electricity influence each other (Jonas et al. 2019).

A heat transfer cooling fluid (normal water with a percentage of an anti-freeze fluid) is used in PVT systems to recover the excess thermal energy generated by the PV cells, hence increasing the electrical conversion efficiency of the collector (Helmers and Kramer 2013). PVT systems, on the other hand, are limited to work at low temperatures (30-80°C), making them appropriate for domestic hot water heating (DHW) (Miljkovic et al. 2011). PVT collectors can be categorized according to their specific operating temperature ranges, system layout, design (glazed, unglazed, and concentrating), and heat transfer medium (air and water, for commercial systems) (Zondag 2008). These systems can be based on concentration (e.g. Compound Parabolic Collector, CPC) or non-concentration configurations. For instance, for low concentration ratios and truncated optics, CPC is a reflector geometry that can concentrate a significant amount of solar radiation towards the receiver without necessarily requiring tracking. There is little research on Low Concentrating Photovoltaic-Thermal (LCPVT) available due to the difficulty of integrating concentrating systems with PV cells (Joshi and Dhoble 2018a). (Koronaki and Nitsas 2018) revealed one of the few situations in which the optical and electrical efficiencies are proven to be about 34% and 15%, respectively. Furthermore, the Incidence Angle Modifier (IAM) presented by them shows that this type of CPC is highly sensitive to specific incident angles. It should be considered that lowering the receiver area in concentrating stationary collectors causes reflection losses and a penalty in IAM. (Sharaf and Orhan 2015) studied PVT (CPVT) systems, and the goal was to combine concentrators with PV and thermal energy. This system is categorized into low, medium, or high concentration ratio technologies; also, it is possible to be stationary or be coupled with a tracking system. (Lämmle et al. 2016) investigated that combining the thermal and electrical systems into a single system optimizes the use of solar resources. By that, area dedicated to solar energy production could be decreased. However, this technology still has some challenges that need to be overcome before using it on a large and commercial scale. One of these challenges is partial shading which (Decker and Jahn 1997) have investigated. Furthermore, (Bunthof et al. 2016) showed that partial shadowing is the primary parameter for decreasing the energy yield of PV arrays. (Woyte, Belmans, and Nijs 2003) studied one possible solution to overcome this challenge by using bypass diodes which allow PV arrays to produce at a lower capacity. In this method, electrical current flows in a different path, and this causes a minor fraction of the total power. (Bunthof et al. 2016) conducted a study that shows costs of the solar collectors increased by adding bypass diodes to the PV arrays. Considering all these parameters, this study focuses on a PVT receiver without a bypass system.

(Cheng et al. 2010) studied fixed CPVT (either in one or two dimensions), and in this study, irradiation distribution on the receiver is considered to be uniform. It should be considered, most concentrating solar collectors mainly provide a non-uniform flux distribution and due to this problem, asymmetric heating patterns create hot spots on the PV cells. To predict the energy output of various solar thermal systems, information on the thermal performance of a wide scope of available solar collector technologies is of extreme importance. Several standards are available to assess the solar thermal collector efficiency, regardless of the technology. Two kinds of tests are possible: the steady or quasi steady-state test and the quasi-dynamic test. For liquid heating collectors, use as a base for their thermal output calculations both models presented in ISO 9806:2017. An electrical performance model based on the work developed by (Lämmle et al. 2017) is available.

2. Electrical and Thermal performance model

2.1 Electrical performance model

To calculate the electrical performance of DM-CPVT, a simplified electrical performance model based on the work developed by (Lämmle et al. 2017) has been employed. The model considers the instantaneous performance ratio (PR) due to incidence angle losses, being expressed by **eq.** 1 for θ greater than zero (Duffie and Beckman 2013).

$$PR_{IAM} = 1 - b_0 \cdot \left(\frac{1}{\cos\theta} - 1\right) \quad \textbf{eq. 1}$$

Where b_0 is the constant for the incident angle modifier. Make it more understandable, the cell temperature $t_{cell,\ PVT}$ was replaced by the fluid mean temperature t_m due to lack of knowledge regarding the solar cell temperature behavior (in relation with the fluid temperature), thus the temperature dependence of the electrical efficiency is expressed by **eq. 2** (Skoplaki and Palyvos 2009).

$$PR_T = 1 - \beta \cdot (t_m - t_{ref}) \quad \textbf{eq. 2}$$

Where t_{ref} is the reference temperature. Due to the selected concentration factor, the low irradiance behavior PR_G presented by (Heydenreich, Müller, and Reise 2008) was not considered, thus the instantaneous specific electrical power output P_{el} is given by the following **eq.** 3 (Lämmle et al. 2017).

$$P_{el} = \eta_{el,STC} \cdot PR_{IAM} \cdot PR_T \cdot G \quad \textbf{eq. 3}$$

Where the temperature coefficient of electrical power β was set to 0.4%/K (Aste et al. 2016) and the standard panel efficiency $\eta_{el,STC}$ to 10%.

2.2. Thermal performance model

To estimate the constant parameters of the collector performance equation, the results have been analysed. The equation is shown in

$$\dot{Q} = A_G[\eta_0 G_{hem} - a_1(T_m - T_a) - a_2(T_m - T_\alpha)^2 - \alpha_8(T_m - T_a)^4] \quad \textbf{eq. 4}$$

In this equation, $\dot{Q}$ is the heat gain which is calculated by the test data, A_g is the gross area, $n_{0,hem}$ is the peak collector efficiency based on hemispherical irradiance G, on the collector surface, a_1, a_2, and a_8 are the loss parameters (defined through this process), T_m is the mean collector temperature, and T_a is the ambient temperature.
In the above equation, the parameters a_2 and a_8 are very small and lower than three times the standard deviation and thus can be omitted. In **eq.** 4, regarding the order of each equation the specific heat gain is given, respectively, once the incident angle modifiers have been set to unity, which is valid for the collector at tracking mode.

$$\frac{Q}{A_g} = \eta_0 G_{hem} - U(T_m - T_a) \quad \textbf{eq. 5}$$

$$\frac{Q}{A_g} = \eta_0 G_{hem} - a_1(T_m - T_a) - a_2(T_m - T_a)^2 \quad \textbf{eq. 6}$$

$$\frac{Q}{A_g} = \eta_0 G_{hem} - a_1(T_m - T_a) - a_2(T_m - T_a)^2 - a_8(T_m - T_a)^4 \quad \textbf{eq. 7}$$

According to the international standard ISO 9806:2017, a Steady-State testing procedure has been planned and done, which were further normalized to the gross area of the specific DM-CPVT.

3. CPVT Collector Design

DM-CPVT is a concentrating, hybrid solar photovoltaic and solar thermal collector (CPVT), which generates both electricity and heat from the same gross area. The collector reflects and concentrates the incoming sunlight, from its reflective mirrors to the bottom side of a (horizontally placed) PVT receiver. This reflector geometry is based on a MaReCo and CPC geometry that has been presented previously by (Cabral et al., 2019). For the DM reflector geometry, in this study, the receiver placement has been kept constant with a gap between the top of the receiver and the glass of 33 mm (Figure 1).

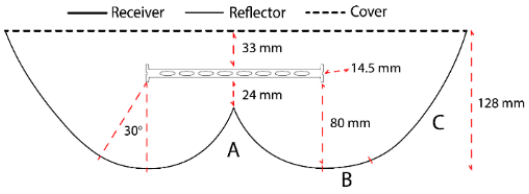

Figure 1. Cross-section view (with dimensions) of the general DM geometries. Circular sections A and B with 80 mm radius and an air gap of 33 mm. A (71° circular section); B (30° circular section); C (parabola section).

This gap has been implemented to reduce convection losses (Duffie and Beckman 2013). An additional gap of around 24 mm has been considered to evenly distribute the reflected sunlight on the bottom side of the receiver. The collector and reflector length were set to 2350 mm, to cope with the shadow created by the lack of reflector in the longitudinal direction. The geometry has an arc angle of around 101° (section A: 71°; section B: 30°). The 30° arc angle employed in the circular section B, has the aim to compensate the Earths' declination (± 23.45°) so that the collector has a wider range of working hours. Information on the main parameters for DM geometry design are presented in the following Table 1.

Table 1. Summary of the main parameters for DM geometry design concept.

Geometry	Concentration factor (C_i)	Reflector depth (z) [mm]	Receiver dimensions (L/W/T) [mm]	Air gap[1] [mm]	Gap[2] [mm]	Radius [mm]	Acceptance half-angle (θ_c) [°]	Circular section arc-angles [°]
DM-CPC	1.3	128	2310/165/14.5	33	24	80	23	101° (71°+30°)

To cope with the short spectral response of monocrystalline silicon solar cell, a reflector from Almeco (Solar Vega SP295f) with an electrical spectral reflectivity in the visible range of ρ= 95 % and a specular reflectance ≥ 91 % has been selected. Furthermore, the total solar reflectance is 92 % with a length of around 2350 mm. The Solarus Sunpower bifacial PVT receiver has been used and has a receiver core with 2310 mm of length, a width of 165 mm and 14.5 mm of thickness. The cell string layout has a length of 2100 mm which comprises 38 one-third-size PV cells (to lower the amount of current in each cell) divided into 4 sub-strings (each one with one diode) of 8-11-11-8 PV cells. The PV cells are encapsulated in a silicone gel from Wacker-Elastosil Solar 2205 with a total thickness of 3.5 mm, with a reported thermal conductivity of 0.2 W/m.K and light transmittance of 97 %.
The PVT absorber has 8 elliptical channels to increase the heat transfer between the aluminum receiver core and the Heat transfer Fluid (HTF), increasing this way the HTF temperature and at the same time lowering the PV cell overall temperature, and thus enhancing the electrical efficiency. The electrical power output of PV modules can be improved by employing smaller sized silicon solar cells as it can effectively reduce the series resistance loss due to lower cell-to-module losses (Haedrich et al. 2014). The selected PV cells from Lightway Solar are characterized by an electrical efficiency of 20.1 %, theoretical maximum output power (P_{mpp}) of 1.57 W, short-circuit current (I_{sc}) of 3.13 A, open-circuit voltage (V_{oc}) of 0.63 V and temperature coefficient of -0.37 %/°C. By having three quarters-size PV cells, the P_{mpp} and I_{sc} should be equal to one-third of the corresponding full-size cells, whereas the V_{oc} should remain the same. Furthermore, a low iron solar glass cover (from Scheuten Glas) and a Plexiglas side gable protection with a thickness of 4 mm have been added to the collector design concept. The emissivity, thermal conductivity and transmittance of glass cover are 84 %, 1 W/m.K and 91 %, respectively. For Plexiglas side gable protection above mentioned values are 94 %, 0.18 W/m.K and 92 %, respectively.

4. Description of Testing Facilities

4.1. Solar Laboratory of University of Gävle (HiG) (Sweden)

The DM-CPVT has been evaluated, built, and installed in the outdoor testing laboratory with a variable south-oriented collector tilt angle (β) depending on the nature of the tests. The test setup apparatus consists of a solar collector closed-loop and a domestic hot water open-loop. Furthermore, the solar collector loop relates to the HTF

[1] Distance between top receiver side and glass cover.
[2] Distance between the bottom receiver side and the mid reflector (middle of section A).

flowing between the collector and heat exchanger, supplied by a fixed flow rate. A mixture of 80% of pure water and 20% of ethylene glycol (with a heat capacity of 2200 J/kg.K) has been used as HTF (overall heat capacity of 3813 J/kg.K). The test stand consists of a hydraulic and electric circuit designed for performance characterization and has been used for both electrical and thermal measurements which measures inlet, outlet and ambient temperature, pressure, flow rate, and global and diffuse solar radiation. The closed-loop is composed of programmable logic controller, automated flow control, collector inlet temperature control, temperature measurement tool, vacuum degasser and stainless-steel piping. The solar collector test facility is composed of a hydraulic and electric circuit designed for domestic solar collector thermal and electrical performance characterization. For both electrical and thermal performance characterization, several testing measurement equipments have been used, such as two KippZonen (CMP3 for diffuse and CMP6 for global radiation) pyranometers (installed in the same plane as the solar collector), IV tracer, ambient and HTF temperature sensors, and flowmeters. The testing equipment is connected to a CR1000 datalogger from Campbell Scientific that monitors, records and processes the data with time-step measurements of 30 sec. All the measurements were then treated as 10 minutes average data to compress and increase data accuracy. Figure 2 shows the CPVT solar collector test apparatus located in the Solar Laboratory of the University of Gävle (HiG).

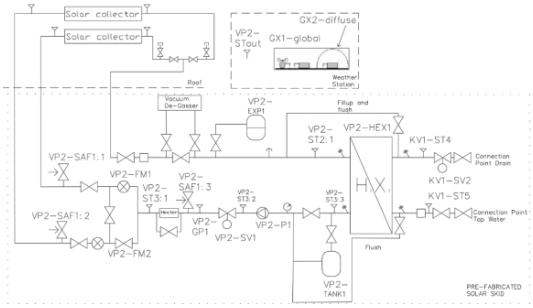

Figure 2. Technical drawing of the hydraulic rig composed of several temperature and pressure sensors.

The hydraulic rig consists of several temperature and pressure sensors, a heat exchanger, a vacuum degasser, an expansion vessel, a mixing tank (for a more homogeneous temperature) and a heater for constant inlet temperature (Figure 2). The setup measures inlet, outlet and ambient temperature, pressure, flow rate, and global and diffuse solar radiation which are for both electrical and thermal measurements. For the thermal performance investigation, in each measurement timetable, the inlet collector temperature was constant (to reach the yield) and the collector's outlet temperature was measured to investigate the collector's thermal function. Table 2 presents both the thermal and electrical measurement components accuracy.

Table 2. Thermal and electrical measurement components and respective accuracy deviation in comparison to the manufacturer datasheets.

Thermal measurement equipment	*Value*	*Accuracy*
Flow rate $\dot{m}$ [L/m]	0.5-10	±1.5 %
Temperature difference ΔT [°C]	0-90	±0.04 %
Pressure interval ΔP [Bar]	Up to 6	±1.5 %
Heater [°C]	10-90	±0.04 %
Pressure transmitter [Bar]	6	±1 %
Electrical measurement equipment	*Data*	*Allowed Deviation*
Pyranometer CMP3 [W/m^2]	Up to 2000	±1.5 %
Pyranometer CMP6 [W/m^2]	Up to 2000	±1 %
IV Tracer [I] [V]	-	0.1 %

4.2. Solar & other Energy Systems Laboratory (SESL) at the NCSRD (Greece)

The DM-CPVT has been moved to Greece at the NCSRD facilities (latitude/longitude: +37°58'/+23°43') for performance assessment during the period of September-October 2020. The test-bench of the PVT collector includes a two-axis tracker, a temperature preparation unit (includes an air-source heat pump and a storage tank) and a pumping station for adjusting the temperature of the heat transfer fluid and fixing the flow rate equipped with several pneumatic valves and mixing circuits. The collector has been mounted and fastened on the tracker with the inlet and

outlet pipes (from one side of the collector) connected with the pumping station. Temperature sensors (4-wire PT100, standard uncertainty 0.05 K) have been installed at the inlet/outlet piping of the collector to measure the water/glycol temperature. These piping parts have been insulated, once the charging and venting processes have been accomplished. An electromagnetic flowmeter with an accuracy of 1% measures the HTF flow rate and two pyranometers (CMP11, accuracy 1.3%) measure the global and diffuse radiation. An IV tracer was used to measure the voltage and current at MPPT conditions. The pressure in the piping was also monitored frequently, to make sure that no air is trapped. The test stand can test (electrical and thermal performance test) at tracking mode, in which the incidence angle does not affect the results (i.e., solar irradiation is always perpendicular to the surface). These tests have been conducted for 5 temperature levels, starting from the ambient (~22 °C) and reaching almost 80 °C. During the tests at each temperature level, the measurements have been recorded, but they have been included in the processing, only when the temperature deviation over a 10-minute duration was less than 0.1 K. This testing protocol is based on the ISO 9806:2017 standard testing specifications for solar thermal collectors and practically ensures a steady-state test and increased reliability. The tests at each temperature level have been finished once 4 of these 10-minute periods were achieved for each level, with the measurements then filtered and averaged. Figure 3 shows the CPVT solar collector test apparatus located in NCSRD (Greece) and the Solar Laboratory of the University of Gävle (HiG, Sweden).

Figure 3. CPVT solar collector test apparatus is located in the Solar Laboratory of the University of Gävle (left image) and at NCSRD (right image).

5. Performance Assessment of DM-CPVT

The electrical performance of the CPVT collector was characterized according to IEC 62108 (2007) in Sweden, while the thermal performance was characterized according to ISO 9806:2017 (by Steady-state (SS) test methods) in Sweden and Greece.

5.1. Thermal & Electrical performance, Sweden

Results from performance assessment in Solar Laboratory of HiG showed that electrical peak efficiency of 10.8% (R^2 = 0.999) for a module temperature of 25 ºC has been achieved. The steady electrical peak efficiency for higher temperatures gives a temperature dependence coefficient of around 0.49 %/ºC. At HiG, the heat loss coefficient U_1, reached a value of 4.48 W/m^2.K, whereas the optical efficiency η_0 reached a value of 63.6 % (divided in 53.1 $\%_{th}$ and 10.5 $\%_{elect}$, R^2 = 0.997) has been obtained per gross area (presented in Figure 4).

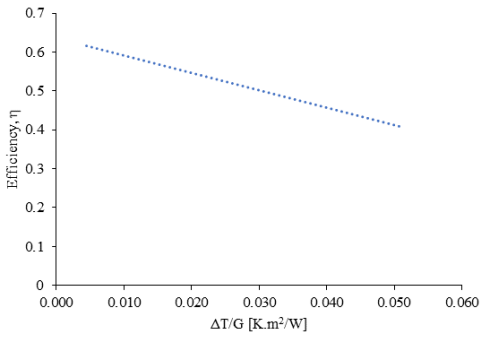

Figure 4. Experimental overall efficiency per gross area measured at HiG, Sweden.

5.2. Thermal performance, Greece

The performance assessment developed at NCSRD showed that the peak thermal power of the collector for beam radiation of 850 W/m^2 and a diffuse radiation of 150 W/m^2 is 1332 W. This power is obtained for a mean collector temperature equal to the ambient temperature (T_m-T_a= 0 K).

The steady-state test method was adopted for the performance tests performed at the NCSRD in Greece. The measured data during the PVT collector tests have been filtered, averaged and presented in five temperature levels in Table 3.

Table 3. Recorded test results of the PVT collector at NCSRD.

T_m (ºC)	G (W/m^2)	G_d (W/m^2)	M (l/h)	T_a (ºC)	T_i (ºC)	T_o (ºC)
26.46	966.5	102.9	198.7	24.9	23.5	29.5
26.60	1004.9	118.5	198.4	24.9	23.5	29.7
26.55	1014.5	144.1	198.7	24.9	23.5	29.6
26.53	996.9	112.6	198.4	24.8	23.5	29.6
39.15	874.3	62.0	196.5	24.4	36.8	41.5
39.12	897.0	63.6	196.4	24.3	36.6	41.6
39.73	1037.8	108.1	194.6	24.9	36.9	42.6
39.50	1044.2	89.2	194.7	24.4	36.6	42.4
48.74	1000.3	69.9	191.9	24.8	46.1	51.3
48.69	989.6	68.3	192.8	24.5	46.1	51.3
50.52	1037.3	75.1	190.7	24.0	47.9	53.2
50.45	1028.3	69.2	190.7	23.8	47.9	53.0
59.89	1006.7	69.6	189.7	25.3	57.6	62.2
60.02	1008.8	67.8	189.2	25.3	57.7	62.4
61.62	971.9	137.0	191.1	21.0	59.5	63.8
61.57	968.4	120.6	191.7	20.9	59.5	63.7
76.46	975.4	112.3	186.8	22.4	74.8	78.1
76.69	1065.3	203.6	187.5	22.6	74.8	78.6
76.70	1068.4	204.9	188.2	22.7	74.8	78.6
76.95	1105.8	257.7	188.2	23.6	75.0	78.9

According to the calculation from the test data, based on the gross area of the collector, the magnitudes of each equation of the thermal performance model are shown in Table 4. A_i is the new reference surface and the values are adjusted and multiplied with the surface ratio A_i/A_G, when the aperture area or the area that would correspond to the commercial product is used.

Table 4. Parameter values and standard deviation of the performance correlation of the PVT collector at NCSRD.

1st Order	Value	Std	Units
$\eta_{0,hem}$	0.515	0.004	-
U_0	4.422	0.136	W/m^{2}K
2nd Order			
$\eta_{0,hem}$	0.505	0.004	-
α_1	3.216	0.371	W/m^{2}K
α_2	0.021	0.006	W/m^{2}K^2
4th Order			
$\eta_{0,hem}$	0.510	0.005	-
α_1	4.536	0.700	W/m^{2}K
α_2	-0.028	0.024	W/m^{2}K^2
α_8	0.000009	0.000004	W/m^{2}K^4

For a parameter to be statistically important, the value of each parameter must be positive and greater than three times its standard deviation (According to the ISO 9806:2017); Therefore the 4th order equation includes a negative a_2 value, which does not have a physical meaning, and on top of that the standard deviation of this parameter is about the same as its value. So, the preferred equation to be used is the 2nd order, which has a good accuracy over the whole range of temperatures tested, from the ambient up to 80 ºC.
The function of the temperature difference based on the test data and the 2nd-order equation as the collector performance is shown in Figure 5 (A).

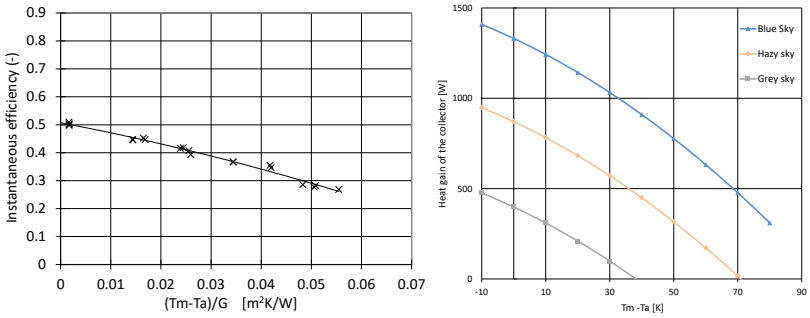

Figure 5. A) Collector performance as a function of the temperature difference at NCSRD (B) Heat gain of the collector for three typical solar irradiation levels at NCSRD.

In addition, the peak thermal power of the collector is 1332 W for beam radiation of 850 W/m^2 and a diffuse radiation of 150 W/m^2. This power is obtained for a mean collector temperature equal to the ambient temperature (T_m-T_a=0 K). Second-order performance correlation of the collector showed that the heat loss coefficient U_1, has a value of 4.42 W/m^2.K and η_0, has a value of 62.7% (divided in 51.9 $\%_{th}$ and 10.8 $\%_{elect}$) based on the gross area, which holds a good accuracy over the whole range of temperatures tested, from the ambient up to 80ºC.
Finally, the procedure of ISO 9806:2017 includes an indicative collector heat gain according to the available solar irradiation, divided into a blue sky, hazy sky and grey sky. Figure 5 (B) shows the heat gain of the collector under these three typical scenarios.

5.3. Electrical performance, Greece

Results from performance assessment in Solar Laboratory of NCSRD showed that electrical peak efficiency of 10.5% (R^2 = 0.999) for a module temperature of 25 ºC has been achieved. When the impact of the IAMs is minimal (they are equal to unity) in tracking mode, the electricity generation is monitored using an IV tracer, which changes the voltage and current to find the condition that produces the peak power. Once the thermal performance has achieved a steady-state condition, this measurement is extremely quick (just a few seconds are required). The tracer sweeps the whole IV curve before identifying the MPPT point. This procedure is performed for each of the collector's four PV rows. The readings of the four IV curves for each row and temperature level are measured in tracking mode.
Figure 6 shows an example of the IV curves, with the MPPT for each of the four PV strings at two temperature levels: ambient and 60°C. It is the ones that are positioned at the rear side of the collector that produces the most power because they receive concentrated solar irradiation.

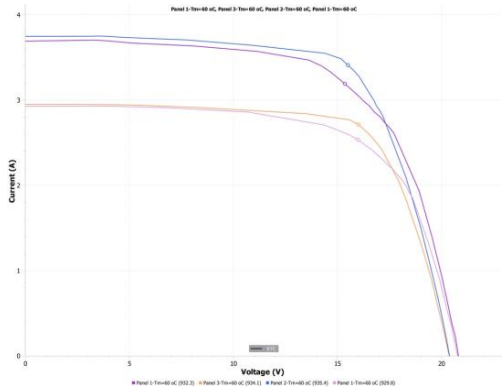

Figure 6. IV curves of the four PV rows of the collector for a temperature level equal to the ambient one (top) and 60 ºC (bottom).

The voltages of the four rows at MPPT are similar, but the currents of the rows positioned on the backside of the receiver are significantly higher. The four panels of the table are labelled as follows:

- Panels 1 & 3 are the back ones (with reflected irradiation);
- Panels 2 & 4 are the front ones (with non-reflected irradiation);
- Panels 1 & 4 are the top ones;
- Panels 2 & 3 are the bottom ones.

Figure 7 shows the test results for the five temperature levels for the PVT collector's electricity production in tracking mode. The measurements at a mean collector temperature of 26 °C were repeated twice to ensure the data's accuracy at this temperature, as the peak electrical power is specified at a similar temperature, which is 25 °C at standard test conditions (STC). The solar irradiation is similar at all temperatures, and that the temperature has a significant impact on the amount of energy produced, as can be seen at all temperature levels. Since solar irradiation is similar for all testing settings, increasing collector temperatures reduce power output almost linearly.

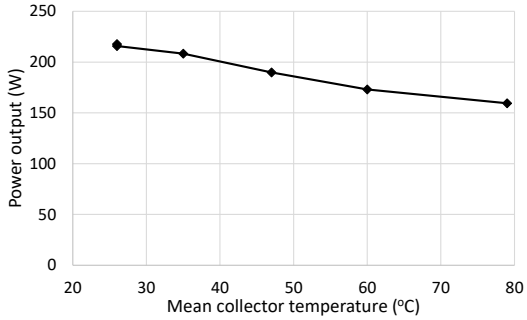

Figure 7.Effect of the collector temperature on the power output.

5.4. IAM tests

To identify the IAMs in both transversal and longitudinal directions, the above performance tests that have been conducted at tracking mode, the collector is adjusted to incidence angles, corresponding to several transversal and longitudinal angles of incidence by the tracker. These are essential to achieve the annual performance of the PVT collector at different angles.

When all IAM values are equal to 1, means that the performance parameters of the collector are fixed with the 2nd-order equation presented previously. For the identification of the IAM values, all tests have been performed during clear days, when the position of the collector was manually varied, to follow the sun movement, and keep either a transversal angle or the longitudinal angle equal to zero. To reach a steady-state thermal condition, the collector positioning should be controlled accurately. So when the solar angle and irradiation are more or less constant for 2-3 hours (typically during the noon), which is adequate to reach a steady-state condition.

According to the ISO 9806:2017, here the estimation of a single IAM value has been extended to three transversal and three longitudinal IAM values. For each angle that was swept, the other angle was kept equal to zero. Therefore, the pairs of transversal/longitudinal angle modifiers obtained are 0/30, 0/40, 0/50, 30/0, 40/0, and 50/0 degrees. To evaluate the electrical IAMs, another angle of 15º has been obtained for both directions (0/15 and 15/0 deg.).

The IAM tests have been done on October 14th 2020 in Greece. The thermal performance should be stabilized and reach a steady-state condition for 10 minutes, with the recorded test data during that period further processed. The test data are shown in Table 5.

Table 5. Steady-state test data for the calculation of the thermal IAMs in Greece

Time / duration	Incidence irradiation (W/m^2)	Diffuse irradiation (W/m^2)	Flow rate (l/h)	Ambient temperature (ºC)	Inlet temperature (ºC)	Outlet temperature (ºC)	Angle, θ (deg.)
11:56-12:06	878.1	79.7	199.0	23.1	21.4	26.7	30 trans.
10:06-10:16	858.6	68.2	199.4	21.7	19.5	23.9	30 long.
11:24-11:35	794.9	76.2	199.1	22.8	21.4	26.0	40 trans.
10:45-10:56	801.3	70.0	199.6	22.2	21.1	24.3	40 long.
13:46-13:56	684.2	72.0	194.6	25.4	21.6	25.4	50 trans.
10:24-10:34	698.9	66.6	200.0	22.1	19.4	22.2	50 long.

The thermal IAMs are calculated by eq. 8 and the previous table data. The specific heat capacity (c_p) and the density used to calculate the mass flow rate ($\dot{m}$) correspond to the water/glycol mixture at the mean collector temperature.

$$K_b(\theta) = \frac{\frac{\dot{m} \cdot c_p \cdot (T_o - T_i)}{A_g} + \alpha_1 \cdot (T_m - T_a) + \alpha_2 \cdot (T_m - T_a)^2}{G \cdot \eta_{0,hem}} \quad \textbf{eq. 8}$$

The resulting thermal IAMs for both transversal and longitudinal directions based on the test data are shown in the following Figure 8.

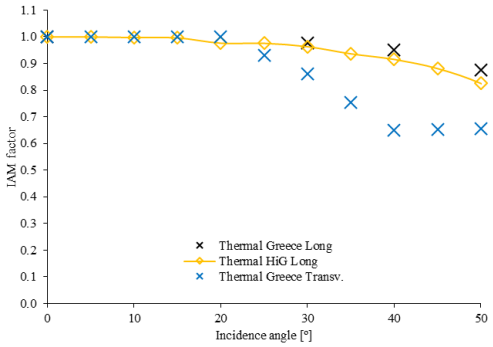

Figure 8. Thermal IAMs (longitudinal and transversal) based on test data direction for both HiG (Sweden) and NCSRD (Greece) laboratories.

In Figure 9 are shown the IAMs for the transversal and longitudinal angles and a standard calculation formula suggested by Ambrosetti (Rasmussen et al. 2020): $K_b(\theta) = 1 - \tan^k\left(\frac{\theta}{2}\right)$, where the parameter *k* determines the slope of the function. This parameter is the average from the ones calculated based on the experimental values, using eq. 9, and is equal to 2.85 for the transversal and equal to 1.267 for the longitudinal angle.

$$k = \frac{\ln(1 - K(\theta))}{\ln\left(\tan\left(\frac{\theta}{2}\right)\right)} \quad \textbf{eq. 9}$$

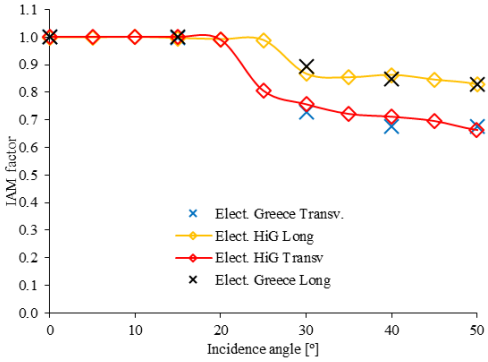

Figure 9. Electrical IAMs for the transversal and the longitudinal direction for both HiG (Sweden) and NCSRD (Greece) laboratories.

The correlation presented in Figure 9 for both testing results in Sweden and Greece, shows a minor deviation in the transversal direction around 20-30º as it falls under the acceptance angle of the CPC reflector geometry. Nevertheless, the agreement is almost perfect between a tracking system used at NCSRD and a hydraulic manual system at HiG. The longitudinal angle closely follows a symmetric profile and can be very well approximated by the Ambrosetti formula with the parameter *k* of 2.85. This formula can be then used to calculate the IAM at the transversal direction for the whole range of incidence angles with very good accuracy.
However, the longitudinal IAMs follow a different pattern due to the concentrator that introduces asymmetric effects, with the available IAMs at that direction used to validate a ray-tracing model of the collector, and thus expand the calculation method over the whole range of angles. In eq. 10 and eq. 11, the diffuse incidence angle modifier constant (K_d) is calculated.

$$K_d = \frac{1}{W} \sum_{\theta,\gamma=0^o}^{90^o} K_{b(\theta,\gamma)} \cdot \sin(\theta) \cdot \cos(\gamma) \quad \textbf{eq. 10}$$

$$W = \sum_{\theta,\gamma=0^o}^{90^o} \sin(\theta) \cdot \cos(\gamma) \quad \textbf{eq. 11}$$

Where K_d is 0.717.

6. Conclusions

DM-CPVT collector geometry showed to be the most promising geometry due to the lower shading impact of this geometry at incidence angles higher than 45º. Moreover, the study showed that the longitudinal direction is closely related to the shading effect, as partial shadowing is substantial from 30˚ onwards. It is important to state that in a PVT collector with concentration, it is necessary to 'sacrifice' (to some extent) the thermal yield to increase the electrical yield, and for this reason, geometry DM-CPVT collector geometry has been the recommended geometry for the CPVT solar collector.

The electrical performance of the CPVT collector was characterized according to the international standards presented in the IEC 62108 (2007), while the thermal performance was characterized according to ISO 9806:2017 (by Steady-state (SS) test methods). Results from performance assessment in Solar Laboratory of both HiG and NCSRD showed that electrical peak efficiencies of 10.8% and 10.5% (R^2 = 0.999) for a module temperature of 25 ºC have been achieved, respectively. The steady electrical peak efficiency for higher temperatures gives a temperature dependence coefficient of around 0.49 %/ºC. At HiG, the heat loss coefficient U_1, reached a value of 4.48 W/m^2.K, whereas the optical efficiency η_0 reached a value of 63.6 % (divided in 53.1 $\%_{th}$ and 10.5 $\%_{elect}$, R^2 = 0.997) has been obtained per gross area. Results from performance assessment at NCSRD showed that the peak thermal power of the collector for beam radiation of 850 W/m^2 and a diffuse radiation of 150 W/m^2 is 1332 W. This power is obtained for a mean collector temperature equal to the ambient temperature (T_m-T_a= 0 K). Second-order performance correlation of the collector showed that the heat loss coefficient U_1, has a value of 4.42 W/m^2.K and η_0, has a value of 62.7% (divided in 51.9 $\%_{th}$ and 10.8 $\%_{elect}$) based on the gross area, which holds a good accuracy over the whole range of temperatures tested, from the ambient up to 80ºC.

7. Acknowledgments

This work has been performed within the RES4BUILD project (Renewables for clean energy buildings in a future power system) – Horizon 2020 program, Grant Agreement no. 814865. The authors would like to express their gratitude to Razif Kunjumon from MG Sustainable Engineering AB for his useful help and discussion during the project.

8. References

Aste, Niccolò, Claudio Del Pero, Fabrizio Leonforte, and Massimiliano Manfren. 2016. "Performance Monitoring and Modeling of an Uncovered Photovoltaic-Thermal (PVT) Water Collector." *Solar Energy* 135:551–68.

Bunthof, L. A. A., F. P. M. Kreuwel, A. Kaldenhoven, S. Kin, W. H. M. Corbeek, G. J. Bauhuis, E. Vlieg, and J. J. Schermer. 2016. "Impact of Shading on a Flat CPV System for Façade Integration." *Solar Energy* 140.

Charron, Remi, and Andreas K. Athienitis. 2006. "Optimization of the Performance of Double-Facades with Integrated Photovoltaic Panels and Motorized Blinds." *Solar Energy* 80(5):482–91.

Cheng, Z. D., Y. L. He, Jie Xiao, Y. B. Tao, and R. J. Xu. 2010. "Three-Dimensional Numerical Study of Heat Transfer Characteristics in the Receiver Tube of Parabolic Trough Solar Collector." *International Communications in Heat and Mass Transfer* 37(7):782–87.

Decker, B., and U. Jahn. 1997. "Performance of 170 Grid Connected PV Plants in Northern Germany—Analysis of Yields and Optimization Potentials." *Solar Energy* 59(4–6).

Duffie, John A., and William A. Beckman. 2013. *Solar Engineering of Thermal Processes*. John Wiley & Sons.

Dwivedi, Pushpendu, K. Sudhakar, Archana Soni, E. Solomin, and I. Kirpichnikova. 2020. "Advanced Cooling Techniques of PV Modules: A State of Art." *Case Studies in Thermal Engineering* 21:100674.

Gomes, João, Linkesh Diwan, Ricardo Bernardo, and Björn Karlsson. 2014. “Minimizing the Impact of Shading at Oblique Solar Angles in a Fully Enclosed Asymmetric Concentrating PVT Collector.” *Energy Procedia* 57:2176–85.

Guarracino, Ilaria, James Freeman, Alba Ramos, Soteris A. Kalogirou, Nicholas J. Ekins-Daukes, and Christos N. Markides. 2019. “Systematic Testing of Hybrid PV-Thermal (PVT) Solar Collectors in Steady-State and Dynamic Outdoor Conditions.” *Applied Energy* 240:1014–30.

Haedrich, Ingrid, Ulrich Eitner, Martin Wiese, and Harry Wirth. 2014. “Unified Methodology for Determining CTM Ratios: Systematic Prediction of Module Power.” *Solar Energy Materials and Solar Cells* 131:14–23.

Helmers, Henning, and Korbinian Kramer. 2013. “Multi-Linear Performance Model for Hybrid (C)PVT Solar Collectors.” *Solar Energy* 92.

Heydenreich, Wolfgang, Björn Müller, and Christian Reise. 2008. “Describing the World with Three Parameters: A New Approach to PV Module Power Modelling.” Pp. 2786–89 in *23rd European PV Solar Energy Conference and Exhibition (EU PVSEC)*.

Jonas, Danny, Manuel Lämmle, Danjana Theis, Sebastian Schneider, and Georg Frey. 2019. “Performance Modeling of PVT Collectors: Implementation, Validation and Parameter Identification Approach Using TRNSYS.” *Solar Energy* 193:51–64.

Joshi, Sandeep S., and Ashwinkumar S. Dhoble. 2018a. “Analytical Approach for Performance Estimation of BSPVT System with Liquid Spectrum Filters.” *Energy* 157.

Joshi, Sandeep S., and Ashwinkumar S. Dhoble. 2018b. “Photovoltaic-Thermal Systems (PVT): Technology Review and Future Trends.” *Renewable and Sustainable Energy Reviews* 92:848–82.

de Keizer, Corry, Minne de Jong, Tiago Mendes, Munish Katiyar, Wiep Folkerts, Camilo Rindt, and Herbert Zondag. 2016. “Evaluating the Thermal and Electrical Performance of Several Uncovered PVT Collectors with a Field Test.” *Energy Procedia* 91:20–26.

Kenny, Robert P., Gabi Friesen, Domenico Chianese, Angelo Bernasconi, and Ewan D. Dunlop. 2003. “Energy Rating of PV Modules: Comparison of Methods and Approach.” Pp. 2015–18 in *3rd World Conference onPhotovoltaic Energy Conversion, 2003. Proceedings of*. Vol. 2. IEEE.

Koronaki, I. P., and M. T. Nitsas. 2018. “Experimental and Theoretical Performance Investigation of Asymmetric Photovoltaic/Thermal Hybrid Solar Collectors Connected in Series.” *Renewable Energy* 118.

Lämmle, Manuel, Thomas Kroyer, Stefan Fortuin, Martin Wiese, and Michael Hermann. 2016. “Development and Modelling of Highly-Efficient PVT Collectors with Low-Emissivity Coatings.” *Solar Energy* 130:161–73.

Lämmle, Manuel, Axel Oliva, Michael Hermann, Korbinian Kramer, and Wolfgang Kramer. 2017. “PVT Collector Technologies in Solar Thermal Systems: A Systematic Assessment of Electrical and Thermal Yields with the Novel Characteristic Temperature Approach.” *Solar Energy* 155:867–79.

Maatallah, Taher, Richu Zachariah, and Fahad Gallab Al-Amri. 2019. “Exergo-Economic Analysis of a Serpentine Flow Type Water Based Photovoltaic Thermal System with Phase Change Material (PVT-PCM/Water).” *Solar Energy* 193:195–204.

Miljkovic, Nenad, Ryan Enright, Shalabh C. Maroo, H. Jeremy Cho, and Evelyn N. Wang. 2011. “Liquid Evaporation on Superhydrophobic and Superhydrophilic Nanostructured Surfaces.” *Journal of Heat Transfer* 133(8).

Proell, M., Ha Karrer, C. J. Brabec, and A. Hauer. 2016. “The Influence of CPC Reflectors on the Electrical Incidence Angle Modifier of C-Si Cells in a PVT Hybrid Collector.” *Solar Energy* 126:220–30.

Rasmussen, Christoffer, Linde Frölke, Peder Bacher, Henrik Madsen, and Carsten Rode. 2020. “Semi-Parametric Modelling of Sun Position Dependent Solar Gain Using B-Splines in Grey-Box Models.” *Solar Energy* 195:249–58.

Sharaf, Omar Z., and Mehmet F. Orhan. 2015. “Concentrated Photovoltaic Thermal (CPVT) Solar Collector Systems: Part I–Fundamentals, Design Considerations and Current Technologies.” *Renewable and Sustainable Energy Reviews* 50:1500–1565.

Skoplaki, Elisa, and John A. Palyvos. 2009. “On the Temperature Dependence of Photovoltaic Module Electrical Performance: A Review of Efficiency/Power Correlations.” *Solar Energy* 83(5):614–24.

Sultan, Sakhr M., and M. N. Ervina Efzan. 2018. “Review on Recent Photovoltaic/Thermal (PV/T) Technology Advances and Applications.” *Solar Energy* 173:939–54.

Tomar, Vivek, G. N. Tiwari, and T. S. Bhatti. 2017. “Performance of Different Photovoltaic-Thermal (PVT) Configurations Integrated on Prototype Test Cells: An Experimental Approach.” *Energy Conversion and Management* 154:394–419.

Woyte, A., R. Belmans, and J. Nijs. 2003. “Testing the Islanding Protection Function of Photovoltaic Inverters.” *IEEE Transactions on Energy Conversion* 18(1).

Zhang, Xingxing, Xudong Zhao, Stefan Smith, Jihuan Xu, and Xiaotong Yu. 2012. “Review of R&D Progress and Practical Application of the Solar Photovoltaic/Thermal (PV/T) Technologies.” *Renewable and Sustainable Energy Reviews* 16(1):599–617.

Zondag, H. A. 2008. “Flat-Plate PV-Thermal Collectors and Systems: A Review.” *Renewable and Sustainable Energy Reviews* 12(4):891–959.